Applying geochemical and colour properties to quantify sediment sources in a Brazilian semiarid ephemeral river system

Rennan Cabral Nascimento, Angelo Jamil Maia, Ygor Jacques Agra Bezerra da Silva, Fábio Farias Amorim, Clístenes Williams Araújo Do Nascimento, Tales Tiecher, O. Evrard, Adrian L Collins, Caroline Miranda Biondi, Yuri Jacques Agra Bezerra da Silva

Applying geochemical and colour properties to quantify sediment sources in a Brazilian semiarid ephemeral river system

Rennan Cabral Nascimento[a], Angelo Jamil Maia[a], Ygor Jacques Agra Bezerra da Silva[a], Fábio Farias Amorim[a], Clístenes Williams Araújo do Nascimento[a], Tales Tiecher[b], Olivier Evrard[c], Adrian L. Collins[d], Caroline Miranda Biondi[a], Yuri Jacques Agra Bezerra da Silva[e]

[a]Agronomy Department, Federal Rural University of Pernambuco (UFRPE), Dom Manuel de Medeiros Street, s/n - Dois Irmãos, 52171-900 Recife, PE, Brazil
[b]Department of Soil Science, Federal University of Rio Grande do Sul (UFRGS), Interdisciplinary Research Group on Environmental Biogeochemistry (IRGEB), Bento Gonçalves Ave. 7712, 91540-000 Porto Alegre, RS, Brazil
[c]Laboratoire des Sciences du Climat et de l'Environnement (LSCE/IPSL), Unité Mixte de Recherche 8212 (CEA-CNRS-UVSQ), Université Paris-Saclay, Gif-sur-Yvette, France
[d]Net zero and resilient farming, Rothamsted Research, North Wyke, Okehampton EX20 2SB, UK
[e]Agronomy Department, Federal University of Piauí (UFPI), Planalto Horizonte, 64900-000 Bom Jesus, PI, Brazil

Abstract

The Brazilian semiarid is the most densely populated dry region in the world. Although climate change projections underline the need for the creation of integrated strategies to protect water resources in the semiarid, sediment source apportionment data remain scant for this environment. Accordingly, we evaluated sediment source contributions in one of the most relevant Brazilian semiarid catchments by combining geochemical and colour tracer properties. In doing so, we explored the applicability of colour tracers as a low-cost alternative to the use of time-consuming and costly properties, such as geochemical tracers. Two source classification schemes were used based on environmentally contrasting regions within the catchment (upper, middle and lower catchment parts) and land use (Caatinga biome - natural vegetation, unpaved roads, and channel banks). Suspended sediments (SS) and bed sediments (BS) were used as target sediment. A total of 660 individual source material samples were collected and composited. Geochemical and colour tracers were measured on the source and target sediment samples and used as potential fingerprints to discriminate and quantify the sediment source contributions. The geochemical tracers provided weak source discrimination based on land use. However, combining geochemical and colour tracers improved the final outputs. Using the MixSIAR model, the lower catchment contributed more sediment than the other regional sources. The Caatinga (SS = 49%; BS = 47%) contributed more sediment than channel banks (SS = 35%; BS = 39%). Overall, our results suggest that the recovery and conservation of the Caatinga vegetation and the stabilization of channel banks, especially in the lower catchment part, are critical for improving sediment supply control in the

semiarid study basin. More studies are needed to evaluate the conservative behaviour of colour tracers in ephemeral rivers.

Keywords: Drylands; Sediment fingerprinting; Colour tracers; Soil erosion; Climate change; Sediment transport.

1. Introduction

Climate change projections underline the urgency of creating integrated strategies for protecting water resources and guaranteeing the continued development of dry regions (IPCC, 2014). In Brazil, the semiarid region, the most densely populated dry region in the world (Marengo, 2008), covers 982,563 km^2 of the country and is mainly concentrated in the Northeast region. The high spatial and temporal variability of rainfall and the high air temperatures and evapotranspiration rates have led to an historical problem of water availability in this region (Correia, 2011). These background problems draw attention to the necessity of tackling soil erosion and sediment transfer within semiarid catchments since the excessive accumulation of fine-grained sediment threatens water quality and decreases reservoir storage capacity (Ayrault et al., 2014; Simplício et al., 2020). In recent decades, the intense deforestation of native vegetation in Brazilian drylands, triggered by agricultural activities, overgrazing, and coal production, has led to an increase in soil erosion (Medeiros et al., 2014; Tomasella et al., 2018; Neto et al., 2020). Therefore, understanding sediment source apportionment at the catchment scale is crucial for implementing targeted strategies to control the transfer of sediments and associated pollutants to surface waters. The sediment fingerprinting approach has been the most widely used direct means of investigating sediment provenance (Collins et al., 2020). Although this approach has been successfully used in other Brazilian rivers in the subtropics (Minella et al., 2007; Tiecher et al., 2014; Ramon et al., 2020), its application for sediment source apportionment in a Brazilian semiarid ephemeral river system has not been reported yet, representing a significant research gap (Silva et al., 2018a; Collins et al., 2020).

Various properties have been used to achieve sediment source apportionment, such as geochemical elements (Collins et al., 1997; Batista et al. 2019), radionuclides (Walling and Woodward, 1992; Ben Slimane et al., 2016), C and N stable isotopes (Garzon-Garcia et al., 2017; Collins et al., 2019) and spectroscopic properties (Tiecher et al., 2016; Amorim et al., 2021). However, the time and resources required to analyse some of these tracers frequently determine the tracer selection and the ongoing lack of standardization among source fingerprinting procedures continues to hinder the wider application of the fingerprinting approach around the world (Collins et al., 2020). For instance, the use of colour tracers is relatively simple, less time-consuming and associated with a lower cost than other properties. Accordingly, colour has been used as an alternative sediment source tracer in many catchments under humid climates (Martínez-carreras et al., 2010; Tiecher et al., 2015; Amorim et al., 2021; Pulley and Collins, 2021). In contrast, studies reporting the applicability of colour tracers in dry environments remain scarce for fluvial sediment fingerprinting and incipient for aeolian sediments (Pulley and Rowntree, 2016; Nosrati et al., 2020; Nosrati et al., 2021a).

The Ipojuca River is one of the most polluted catchments in Brazil and is largely (~70%) semiarid in nature. Sediment-associated metal concentrations and fluxes in this river are comparable to those observed in drainage systems heavily impacted by mining activities (Silva et al., 2015, 2018b). Bed sediments in the upper catchment (semiarid) exhibit, for instance, high levels of Ni and Zn (Silva et al., 2017). Battery factories, textile industries and some municipalities directly discharge non-treated wastewater into the main watercourse (Lima Barros et al., 2013). In the above context, the current research quantified source contributions to suspended sediments (SS) and bed sediments (BS) using geochemical and colour tracers in this semiarid catchment. In doing so, we explored the applicability of colour parameters as an alternative to geochemical tracers, which can be particularly problematic to use in catchments potentially impacted by substantial anthropogenic pollution.

2. Material and methods

2.1 Study area

The semiarid part of the Ipojuca River basin (Figure 1) comprises an area of approximately 2500 km² (CONDEPE / FIDEM, 2005). The average annual rainfall ranges from 600 to 900 mm with high spatial and temporal variability, leading to an ephemeral and perennial fluvial regime in the upper and middle portions of the catchment, respectively (CONDEPE / FIDEM 2005). Soil parent materials are mainly metalluminous granitoids, orthogneisses and biotite-muscovite gneisses (Silva et al., 2015) (Figure 1). Soils are mostly Entisols, Alfisols, and Ultisols (CONDEPE / FIDEM 2005). The preserved and semi-preserved areas of the Caatinga biome comprise a variety of vegetation species, such as *Mimosa tenuiflora* (Willd.)Poir., *Croton sonderianus Muell*. Arg, *Aspidosperma pyrifolium* Mart., *Combretum leprosum* Mart., *Cenostigma pyramidalis* E, Gagnon & GP Lewis, *Croton sonderianus* Muell. Arg, *Commiphora leptophloeos* (Mart.) JB Gillet, *Anadenanthera colubrina* (Vell.) Brenan, *Cereus jamacaru, Pilosocereus gounellei* and *Prosopis juliflora*. Many of these species have shrubby, thorny structures with twisted trunks and are predominantly hyperxorophilous (i.e., a group of species more resistant to aridity).

2.2 Retrieval of source and target sediment samples

Soil samples (see Figure 1) were collected from the main potential sediment sources. These sources were identified by a preliminary assessment of spatial representativeness using satellite images, soil, geology and slope maps. After that, a ground survey was performed to identify sampling locations hydrologically connected and delivering sediment directly to the main watercourse of the Ipojuca River and important tributaries. A total of 660 individual source samples were collected and composited into 44 source material samples. Each composite source sample was composed of 15 sub-samples collected at 0-5 cm depth for surface sources and from the lower horizons of channel bank profiles. Two source classification schemes were generated based on regional geological characteristics and land uses. The regional classification scheme assumed that different sources can be based on geological contrasts. Here, we divided the basin into three potential regional sources (Figure 1): upper (n = 10), middle (n = 20), and lower (n = 14) catchment. The upper basin is represented geologically by Proterozoic volcano-sedimentary sequences, with a predominance of muscovite-biotite gneisses, metaluminous granitoids and metavolcanic rocks. The middle portion is underlain by a series of alkaline granitic rocks, such as alkali-feldspar granites, syenogranites, monzogranites, monzonites and quartzossienites. The lower basin is predominantly underlain by ortho-derivative gneisses (granodiorite and tonalite) containing amphibolite, migmatite, and metadiorite.

The source material samples were also classified according to land use (Figure 1): topsoils from the Caatinga biome (n = 17), channel banks (n = 20), and unpaved roads (n = 7). *Caatinga* samples represented the preserved and semi-preserved conditions found in the semiarid areas in the basin, and included samples collected under riparian vegetation.

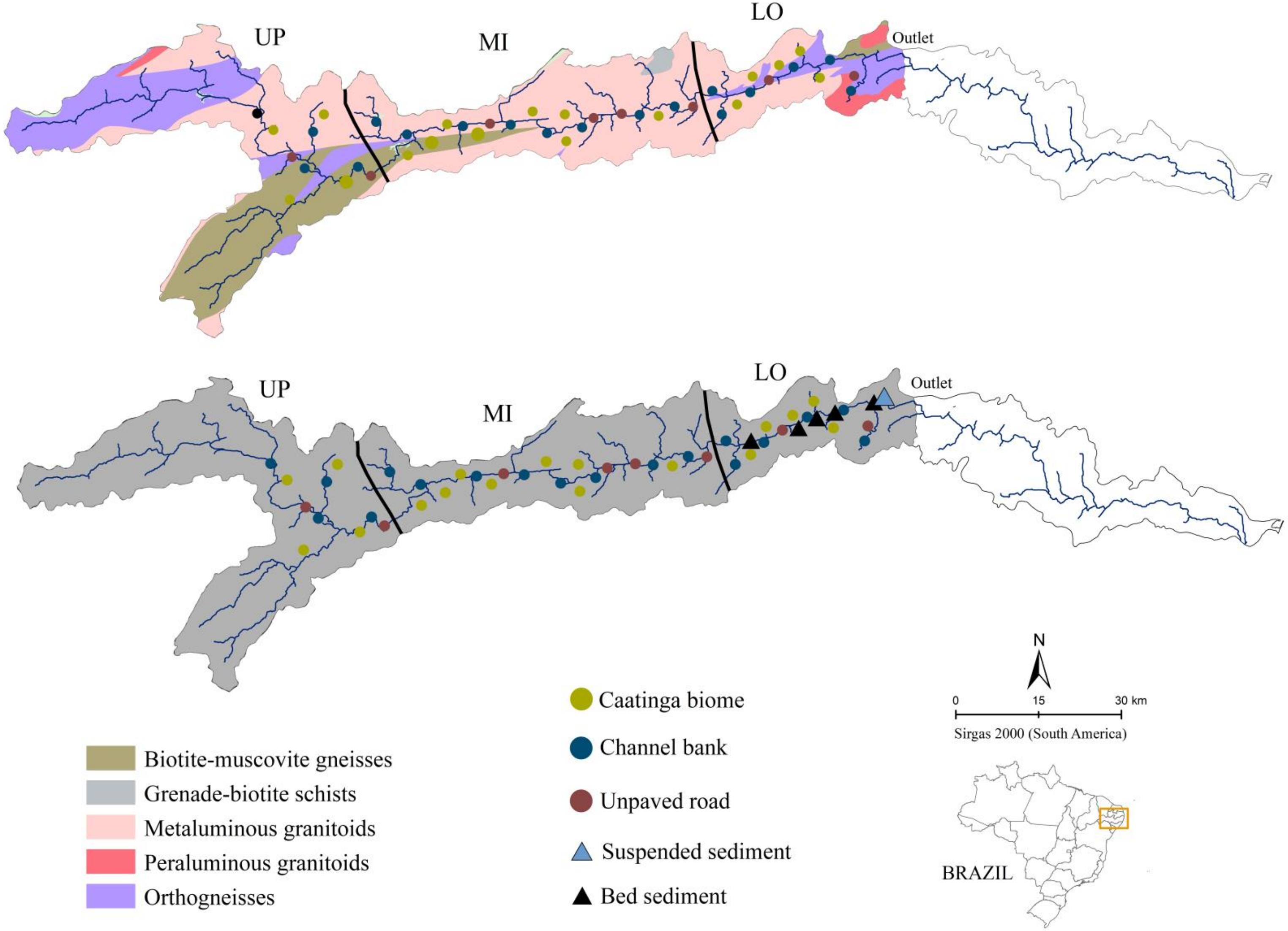
UP
MI
LO
Outlet
UP
MI
LO
Outlet
Biotite-muscovite gneisses
Grenade-biotite schists
Metaluminous granitoids
Peraluminous granitoids
Orthogneisses
Caatinga biome
Channel bank
Unpaved road
Suspended sediment
Bed sediment
N
0
15
30 km
Sirgas 2000 (South America)
BRAZIL

Fig. 1. Location of the study catchment, geology and sampling sites for potential sediment source and target sediment samples. UP = upper catchment, MI = middle catchment, LO = lower catchment.

Target suspended sediment samples (n = 3) were collected from a cross-section in the lowest reach of the study river using time-integrated samplers (Phillips et al., 2000). The suspended sediment samples collected represented material transiting in the river during the periods from May to June 2019 and from June to November 2019. These time periods represented the high and low water discharge periods, respectively. The total rainfall accumulation recorded during the entire observation period was 303 mm (Table S1), similar to the historical pattern observed during previous years in the region. Target bed sediment samples (n = 5) were collected by taking surface scrapes in November 2019 in the lower catchment (Figure 1), exercising care not to exceed 5 cm in depth.

2.3 Geochemical analyses

The source samples were air-dried whereas the target sediment samples were dried in a temperature-controlled circulation oven at 50 °C. All samples were passed through a 32 μm mesh stainless steel sieve, the most important sediment size exported by the main watercourse (Fig. S1). Aliquots (0.5 g each) were first digested in 10 mL of HF in a resting system for 12 h. Subsequently, samples were digested in 5 mL of HNO_3 and 3 mL of $HClO_4$ at 180°C. This last process was repeated to ensure the complete digestion of the samples. Finally, the resulting extract was diluted in 5 mL of HCl (Estévez Alvarez et al., 2001). Standard operation and analytical data quality assurance procedures were followed, including the use of calibration curves, high purity acids, curve recalibration, analysis of reagent blanks, and standard reference materials (SRM 2709 Montana Soil, National Institute of Standards and Technology, NIST, 2002). All analyses were performed in duplicates. Total concentrations of Al, Ba, Ce, Co, Cr, Fe, La, Mn, Nd, Ni, Pb, Pr, Sc, Sm, Sn, Sr, Th, Ti, V, Y, Zn, and Zr were determined by ICP-OES (Optima DV7000, PerkinElmer). In order to improve the sensitivity to metal determination, we coupled a cyclonic spray chamber/nebulizer to the ICP-OES. Recovery rates ranged from 83% to 106%. Total Zr concentrations were determined using portable X-ray fluorescence spectrometry (model S8 TIGER ECO - WDXRF-1KW).

Samples of granite, the most common rock type observed in the Ipojuca River catchment, were collected and the mineralogy analyzed on fine polished sections using a petrographic microscope (Murphy 1986). Mineral identification was carried out using a scanning electron microscopy (SEM; TESCAN, VEGA-3 LMU) at an accelerating voltage of 15 kV. Afterwards, an energy-dispersive X-ray spectroscopy (EDS) detector (Oxford Instrument, model: 51-AD0007) coupled with SEM was used to determine the elemental composition of the mineralogical assembly.

2.4 Colour parameters

The source material and target sediment samples were scanned using a conventional office scanning system - EPSON EcoTank-L355 printer. RGB values were averaged using the GIMP 2.10.22 software tools. Colosol software models (Viscarra Rossel et al., 2004) were used to measure or calculate 24 colour parameters (table 1): Red (R), Green (G), Blue (B), Hue (H_{col}), Value (V_{col}), Chroma (C_{col}), Brightness (Y_{col}), Virtual component X (X), Virtual component Z (Z), Chromatic coordinate x (x), Chromatic coordinate y (y), Dominant wavelength (λd (nm)), Purity of excitation (Pe), Metric lightness function (L), Chromatic coordinate opponent red-green scales (a*), Chromatic coordinate opponent blue-yellow scales (b*), Chromatic coordinate opponent red-green scales (u*), Chromatic coordinate opponent blue-yellow scales (v*), CIE hue (h*), CIE chroma (c*), Hue (H_{RGB}), Light intensity (I_{RGB}), Chromatic information (S_{RGB}), and Redness index (RI).

Table 1. Colour parameters used and their respective calculations used by the ColoSol software.

Colour parameters	Calculation
Red (R)	direct measurement
Green (G)	direct measurement
Blue (B)	direct measurement
Hue (H_{RGB})	$H_{RGB} = \frac{(2.G) - R - G}{4}$
Light intensity (I_{RGB})	$I_{RGB} = \frac{R + G + B}{3}$
Chromatic information (S_{RGB})	$S_{RGB} = \frac{R - B}{2}$
Chromatic coordinate x (x)	$x = \frac{X}{X + Y_{col} + Z}$
Chromatic coordinate y (y)	$y = \frac{Y_{col}}{X + Y_{col} + Z}$
Brightness (Y_{col})	$Y_{col} = 11.396Y_c^{\frac{1}{3}} - 1.610$
Virtual component X (X)	$X = 11.559X_c^{\frac{1}{3}} - 1.695$
Virtual component Z (Z)	$Z = 11.510Z_c^{\frac{1}{3}} - 1.691$

Metric lightness function (L)	$L = 116\,.\left(\frac{Y_{col}}{Y_0}\right)^{\frac{1}{3}}$
Chromatic coordinate opponent red–green scales (u*)	$u^* = 13L\,.(u' - u_n')$
Chromatic coordinate opponent blue–yellow scales (v*)	$v^* = 13L\,.(v' - v_n')$
Chromatic coordinate opponent red–green scales (a*)	$a^* = 500\,.\left[\left(\frac{X}{X_0}\right)^{\frac{1}{3}} - \left(\frac{Y_{col}}{Y_0}\right)^{\frac{1}{3}}\right]$
Chromatic coordinate opponent blue–yellow scales (b*)	$b^* = 500\,.\left[\left(\frac{Y_{col}}{Y_0}\right)^{\frac{1}{3}} - \left(\frac{Z}{Z_0}\right)^{\frac{1}{3}}\right]$
CIE chroma (c*)	$c^* = \sqrt{(a^*)^2 + (b^*)^2}$
CIE hue (h*)	$h^* = arctan\left(\frac{b^*}{a^*}\right)$
Hue (H_{col})	$H_{col} = \left\lvert tan^{-1}\left(\frac{S_2}{S_1}\right).\,\frac{100}{2\pi}\right\rvert$
Value (V_{col})	$V_{col} = f(Y)$
Chroma (C_{col})	$C_{col} = \sqrt{S_1^2 + S_2^2}$
Dominant wavelength (λd (nm))	$P_e = \frac{x - x_w}{y - y_w}$
Purity of excitation (Pe)	$P_e = \frac{x - x_w}{y_b - y_w}$
Redness Index (RI)	$RI = \frac{L((a*)^2 + (b*)^2)^{0.5}.\,10^{8.2}}{b*.\,L^6}$

2.5 Selection of tracers and apportionment of sediment sources

The selection of tracers for final composite fingerprints was undertaken using two steps: (1) assessment of conservative behaviour (i.e., range test), and; (2) linear discriminant function analysis (i.e., forward stepwise procedure). Conservation was tested by comparing the minimum and maximum values of the properties for source and target sediment samples, excluding outliers. Linear discriminant analysis ($p < 0.1$) selected the final set of tracers according to the minimization of Wilks' lambda. The MixSIAR model (Stock and Semmens, 2016) was used to estimate the mean relative source contributions. The Markov Chain Monte Carlo (MCMC) parameters in MixSIAR were set as follows: number of chains = 3; chain length = 100000; burn = 50000; thin = 50. Model outputs were rejected if any variable was above 1.01 for Gelman-Rubin diagnostics. The model prediction accuracies were validated using virtual sediment mixtures, calculated as the product of the known contribution of each individual source and the corresponding average of the tracers measured in that source (Phillips and Gregg, 2003). Here, the mean values of the root mean square error (RMSE) and mean absolute error (MAE) were used as diagnostics for accuracy. All statistical procedures were performed using R software (version 3.6.1, R Core Team, 2021).

3. Results

3.1 Selection of colour and geochemical tracers

The results of the range test for tracer conservation are presented in Figures 2 and 3. Approximately 82% (regional sources) and 64% (land uses) of the geochemical elements passed this test. Non-conservative geochemical tracers were removed from the final discrimination and apportionment modelling for both regional sources (Ce, La, Th, and Zr) and land use sources (Ce, La, Nd, Pr, Sm, Y, Th, and Zr). Among the colour tracers, only H_{RGB}, h*, H_{col} and λd (nm) for the regional sources and Red, H_{RGB}, h*, H_{col}, and λd (nm) for the land use sources passed the range test. Again, only those colour tracers passing the range test were included in the next steps of data processing.

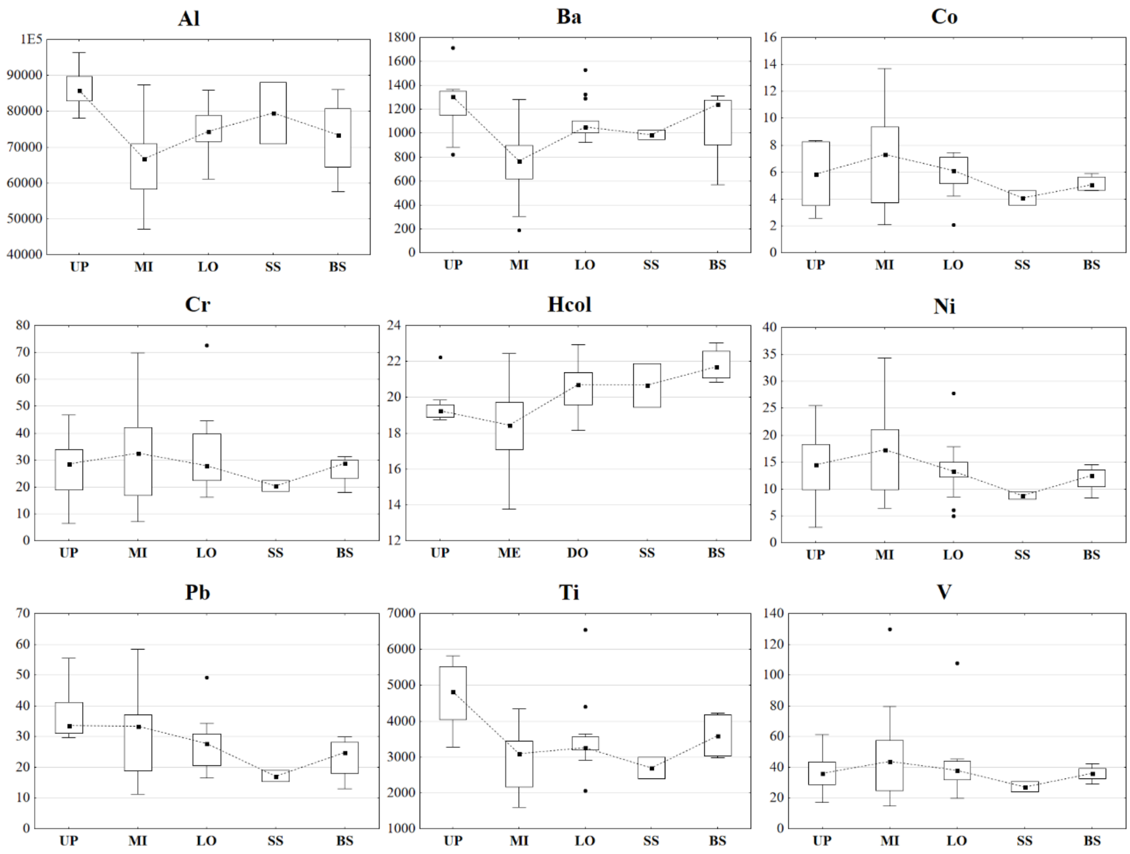

Fig. 2. Boxplots of the geochemical (mg kg^{-1}) and colour tracers passing the conservation test and using the regional sources classification scheme. UP = upper catchment, MI = middle catchment, LO = lower catchment; SS = target suspended sediments; BS = target bed sediments.

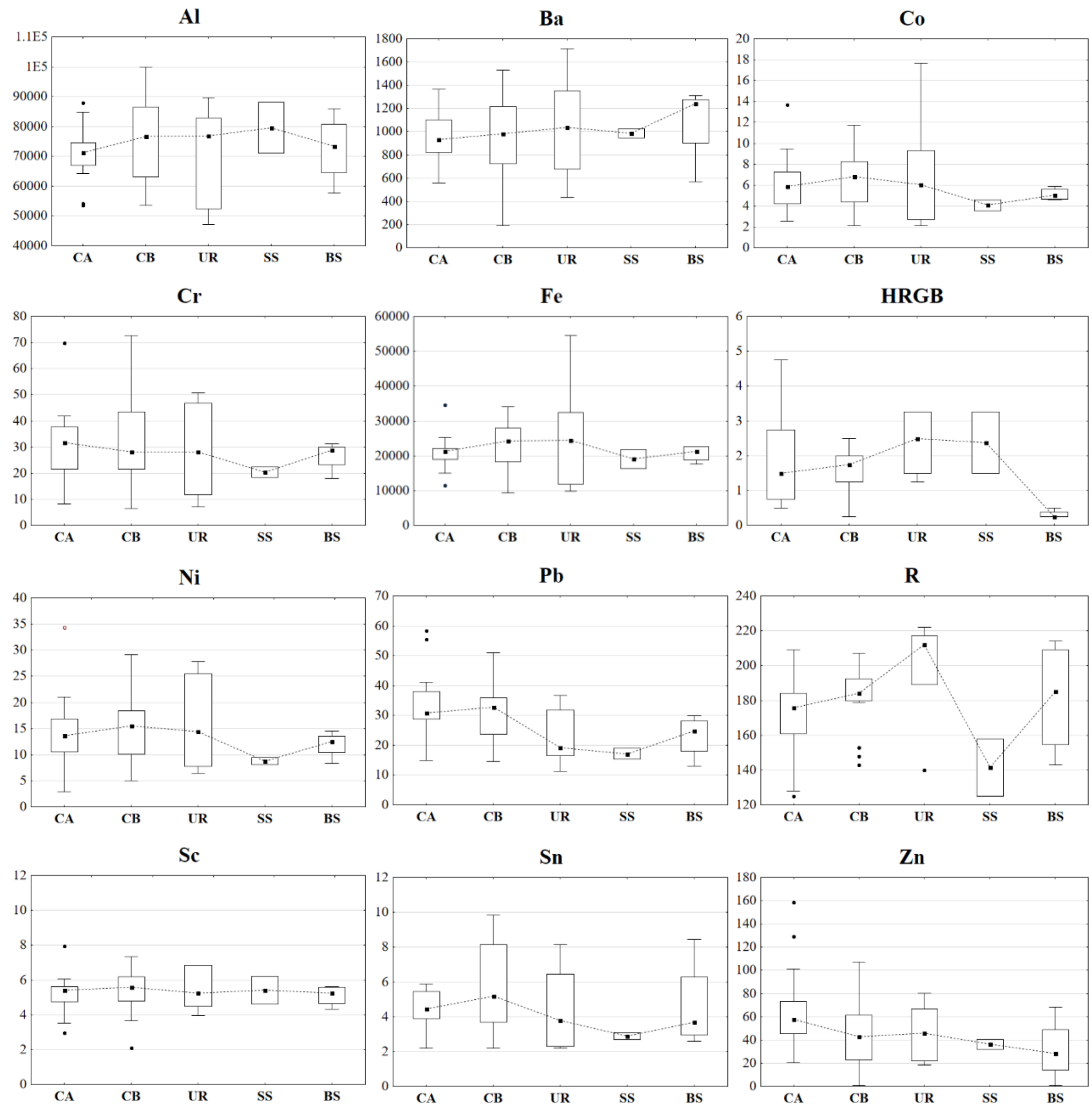

Fig. 3. Boxplots of geochemical (mg kg^{-1}) and colour tracers passing the conservation test and using the land use source classification scheme. CA = Caatinga; CB = channel banks; UR = unpaved roads; SS = target suspended sediments; BS = target bed sediments.

The results of the forward stepwise LDA ($p<0.1$) for regional and land use sources are shown in Tables 2 and 3, respectively. The geochemical tracers alone showed a higher discriminatory power for regional sources (Figs. S2 and S3). The colour parameters alone did not satisfy the minimum requirements for LDA (i.e., the number of approved variables was lower than the number of potential sediment sources), selecting only H_{col} for both source classification schemes, which provided a high percentage of discriminatory error: Wilks' Lambda (WL) = 0.74 and Error rate (ER) = 0.40 (regional sources); WL = 0.78 and ER = 0.46 (land use sources). The final selected geochemical tracers (Ba, Cr, Ti, V, Pb, and Ni) and the final combination of both types of tracers (Ba, H_{col}, Ti, Co, Ni, V, Cr, Pb, and Al) were able to discriminate correctly 98% and 95% of the samples for the regional sediment sources (Table 2). For the land use sediment source classification scheme, the geochemical tracers alone (Fe, Zn, Sn, Sc, Ni, Ba, Al, and Co) and the combination of geochemical and colour tracers (Fe, RED, Ti, Al, Ba, H_{RGB}, Co, Zn, Sn, Sc, Cr, and Pb) correctly classified 82% and 95% of the source material samples, respectively (Table 3).

Table 2. Final composite signatures selected by linear discriminant analysis and corresponding statistical results for the regional sediment source classification scheme for the Ipojuca River catchment.

Tracers	Wilks' lambda	F-value	p-value	p-value (individual)	ER
Geochemical tracers					
Ba	0.50	20.30	<0.01	0.01	0.25
Cr	0.39	11.92	<0.01	0.01	0.18
Ti	0.23	14.17	<0.01	0.01	0.16
V	0.17	13.41	<0.01	0.01	0.11
Pb	0.15	12.02	<0.01	0.04	0.09
Ni	0.10	12.54	<0.01	0.00	0.02
Geochemical tracers + colour tracers					
Ba	0.50	20.30	<0.01	0.01	0.25
H_{col}	0.39	12.22	<0.01	0.01	0.20
Ti	0.30	10.80	<0.01	0.01	0.20
Co	0.15	15.20	<0.01	0.01	0.11
Ni	0.13	13.37	<0.01	0.06	0.07
V	0.10	12.53	<0.01	0.03	0.07
Cr	0.09	11.88	<0.01	0.04	0.05
Pb	0.07	11.56	<0.01	0.04	0.02
Al	0.06	11.15	<0.01	0.06	0.05

ER = error rate; H_{col} (Hue).

Table 3. Final composite signatures selected by linear discriminant analysis and corresponding statistical results for the land use sediment source classification scheme for the Ipojuca River catchment.

Tracers	Wilks' lambda	F-value	p-value	p-value (Individual)	ER
Geochemical elements					
Fe	0.85	3.48	0.04	0.04	0.45
Zn	0.72	3.55	0.01	0.03	0.34
Sn	0.63	3.37	0.01	0.07	0.30
Sc	0.56	3.19	0.01	0.10	0.32
Ni	0.45	3.68	0.01	0.01	0.25
Ba	0.39	3.64	0.01	0.08	0.27
Al	0.31	4.04	0.01	0.02	0.20
Co	0.26	4.05	0.01	0.07	0.18
Geochemical tracers + colour tracers					
Fe	0.85	3.48	3.48	0.04	0.45
RED	0.65	4.88	6.47	<0.01	0.36
Ti	0.52	5.11	4.93	0.01	0.34
Al	0.46	4.57	2.48	0.10	0.32
Ba	0.36	4.94	4.95	0.01	0.32
H_{RGB}	0.29	5.17	4.46	0.02	0.16
Co	0.25	5.01	2.73	0.08	0.14
Zn	0.22	4.90	2.66	0.08	0.14
Sn	0.17	5.26	4.59	0.02	0.11
Sc	0.14	5.47	3.83	0.03	0.05
Cr	0.11	5.51	2.91	0.07	0.07
Pb	0.09	5.49	2.58	0.09	0.05

ER = error rate.

3.2 Sediment source contributions and prediction uncertainties

The average contributions of the regional sources to the two types of target sediment (i.e., SS and BS) were similar, regardless of the tracer set used (Figure 4) and followed the subsequent decreasing contribution order: lower catchment (LO) > upper catchment (UP) > middle catchment (MI). The lower sites showed higher contributions to SS and BS than the middle and upper catchment. Geochemically speaking, the Caatinga was the main land use-based sediment source (SS = 55% and BS = 54%). When using a combination of geochemical and colour tracers, the channel banks (SS = 40% and BS = 45%) and Caatinga (SS = 43% and BS = 41%) showed relatively similar sediment contributions. The middle portion of the study basin and unpaved roads exhibited lower contributions to both SS and BS.

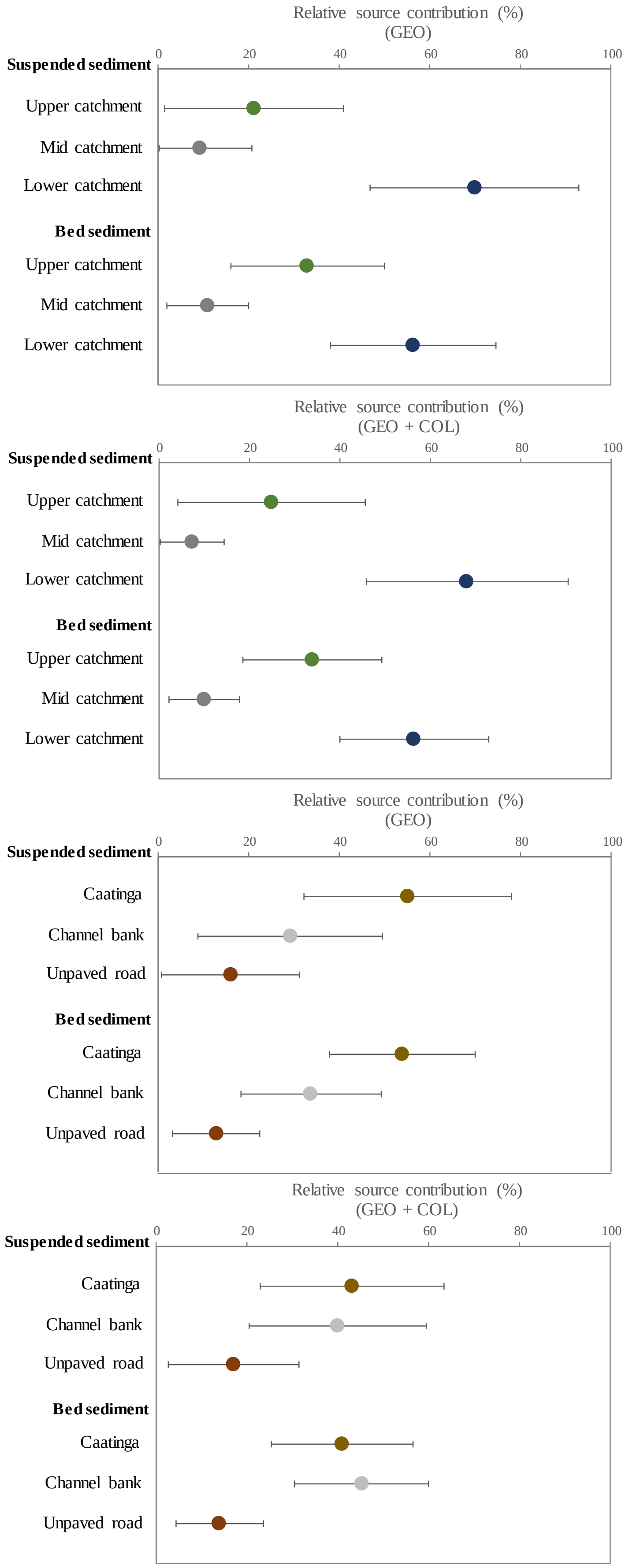
Relative source contribution (%)
(GEO)
0
20
40
60
80
100
Suspended sediment
Upper catchment
Mid catchment
Lower catchment
Bed sediment
Upper catchment
Mid catchment
Lower catchment
Relative source contribution (%)
(GEO + COL)
Suspended sediment
Upper catchment
Mid catchment
Lower catchment
Bed sediment
Upper catchment
Mid catchment
Lower catchment
Relative source contribution (%)
(GEO)
Suspended sediment
Caatinga
Channel bank
Unpaved road
Bed sediment
Caatinga
Channel bank
Unpaved road
Relative source contribution (%)
(GEO + COL)
Suspended sediment
Caatinga
Channel bank
Unpaved road
Bed sediment
Caatinga
Channel bank
Unpaved road

Fig. 4. Mean values and standard deviations for the predicted relative contributions to target suspended sediments and bed sediments using the regional source and land use source classification schemes. GEO = geochemical tracers; GEO + COL = geochemical + colour tracers.

The MixSIAR models used to estimate the sediment source contributions exhibited convergence for the Gelman-Rubin test (<1.01) and sufficiently long Markov chains. The low values for RMSE and MAE indicated that the predicted values were similar to the known virtual mixtures. Therefore, all the modelled source contributions were considered to be acceptably accurate (Table 4). The overall average values of RMSE and MAE were 6.0% and 5.5%, respectively, and these are clearly comparable to the accuracy reported by other studies using sediment source fingerprinting (Uber et al., 2019; Nosrati et al., 2021b; Nosrati et al., 2021c; Amorim et al., 2021).

Table 4. Mean known and predicted relative contributions (and corresponding standard deviations) of the sediment sources to target suspended sediment (SS) and bed sediment (BS) samples and associated accuracies based on the virtual mixture tests.

Sources	Tracers	Target Sediment	Sources	Known mean contribution (%)	SD (%)	Predicted mean contribution (%)	RMSE	MAE
Regional	GEO	SS	UP	21.1	19.8	27.5	7.4	7.0
			MI	9.1	11.6	13.2		
			LO	69.8	23	59.4		
		BS	UP	32.9	16.9	34.8	4.5	4.2
			MI	10.8	9	15.2		
			LO	56.3	18.3	50.1		
	GEO + COL	SS	UP	24.8	20.7	22.7	3.2	3.0
			MI	7.2	8.3	11.7		
			LO	68	22.3	65.6		
		BS	UP	33.8	15.3	24.9	6.6	5.9
			MI	9.9	7.7	11.8		
			LO	56.3	16.4	63.3		
Use	GEO	SS	CA	55	23	46.8	10.3	9.7
			CB	29.1	20.3	43.7		
			UR	15.9	15.2	9.5		
		BS	CA	53.7	16.1	46.5	8.1	7.6
			CB	33.6	15.5	44.9		
			UR	12.8	9.6	8.6		
	GEO + COL	SS	CA	43.1	20.2	34.5	8.1	7.3
			CB	39.9	19.4	50.8		
			UR	17	14.4	14.6		

		CA	40.9	15.6	32.8		
	BS	CB	45.2	14.7	52.6	6.3	5.4
		UR	13.9	9.6	14.6		

GEO = geochemical tracers; GEO + COL = geochemical + colour tracers; UP = upper catchment; MI = middle catchment; LO = lower catchment; CA = Caatinga; CB = channel banks; UR = unpaved roads; standard deviation (SD); root mean squared error (RMSE) and mean absolute error (MAE).

4. Discussion

4.1 Discrimination of regional sources and land uses

In general, the geochemical tracers propagated lower errors for sediment source discrimination and apportionment. This was most notable for the regional sediment source scheme and possibly reflects the exclusive geochemical properties for each part of the study catchment. The average Al, Ba, and Ti concentrations showed the main contrasts between these sources and followed typically the sequence: upper catchment > lower catchment > middle catchment. In the middle portion of the study catchment, the lower Al contents were likely related to the predominance of metalluminous granitoids containing a higher proportion of alkali metals (Figure 5b) in comparison to soils derived from other parent materials (Figures 5a and 5c) (Table 5). The upper catchment exhibits greater geological variation, including for instance the occurrence of orthogneisses, volcano-sedimentary rocks, and intercalations of mafic rocks, mainly amphibolites. The distribution of orthogneiss and volcano-sedimentary rocks are likely responsible for the highest concentrations of Al, Ba, and Ti in the upper catchment. The lower catchment is characterized by orthogneiss with different compositions, such as monzogranitic and granodioritic.

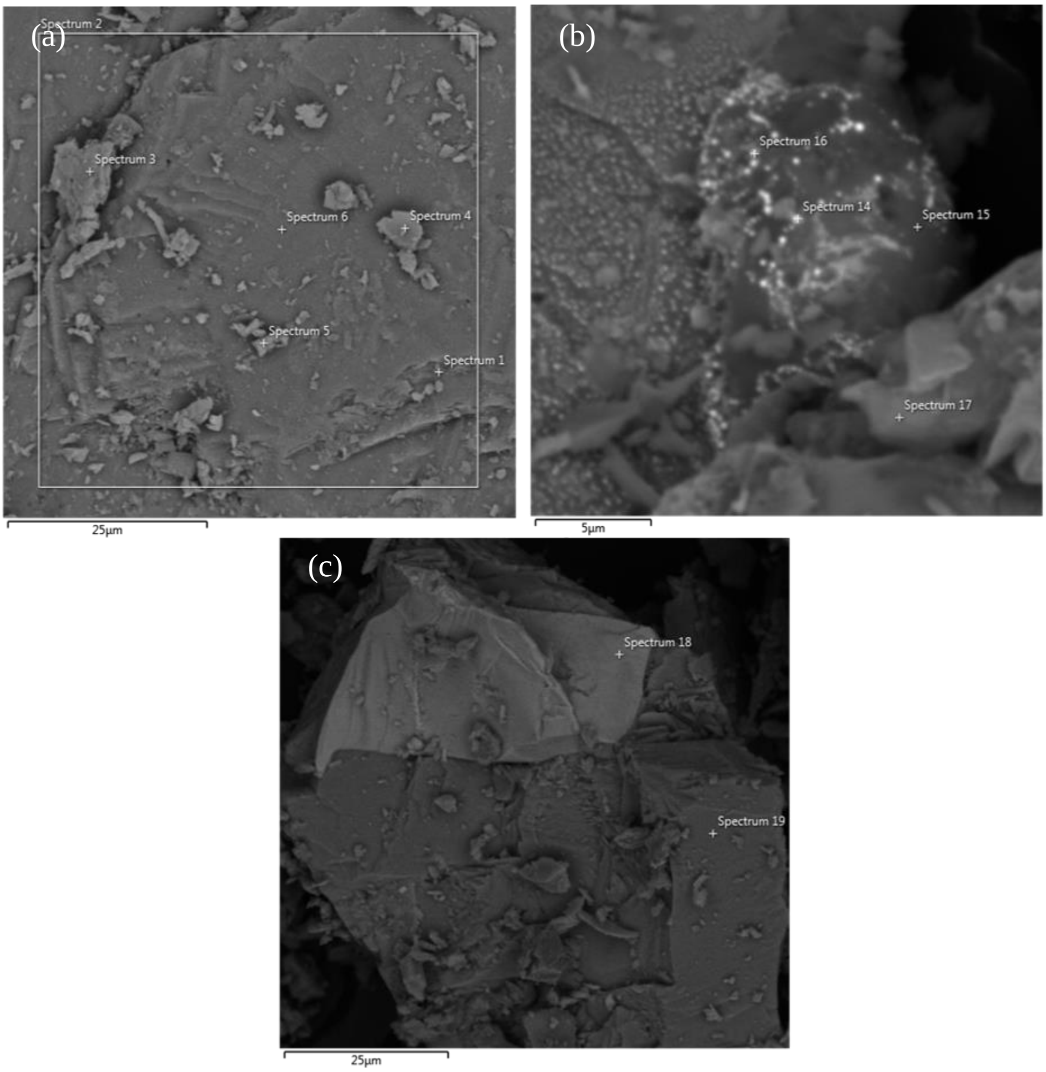

Fig. 5. Cross-sectional images of granites from the Ipojuca River basin using a scanning electron microscope with energy-dispersive X-ray spectroscopy attached facilities (SEMEDS). A) granite from the upper catchment. B) metaluminous granite from the middle catchment. C) granite from the upper catchment.

Table 5. Elemental composition of minerals in granites in the Ipojuca River watershed, using a scanning electron microscope with energy-dispersive X-ray spectroscopy attached facilities (SEM-EDS).

Elements	C	O	Na	Mg	Al	Si	K	Ca	Fe	Ba
Granite from the upper catchment (a) (%)										
Spectrum 1		43.7	0.9		9.4	27.7	10.8		0.4	0.5
Metaluminous granite from the mid catchment (b) (%)										
Spectrum 14		22.3		2.2	3.3	7.3	3.6		4.9	
Spectrum 15	7.9	21.4	0.5	2.2	6.0	17.5	12.6	1.4	25.7	
Spectrum 16	6.4	25.7	1.0	1.8	5.6	16.3	9.9	1.1	16.7	
Spectrum 17	15.7	34.4	0.9	3.0	5.4	12.3	5.6	0.5	13.9	
Granite from the upper catchment (c) (%)										
Spectrum 19			1.7	11.2	9.6	39.4	1.5		22.5	

Unlike the geochemical tracers, the colour parameters showed poor conservative behaviour (82% failed the range test). The high input of organic waste observed in the Ipojuca River basin (Lima Barros et al., 2013) and the particle size fraction used (<32 µm) might have combined via the enrichment of sediment in organic matter to reduce the discriminatory efficiency of colour parameters (Pulley and Rowntree, 2016; Pulley and Collins, 2022). When combined with geochemical parameters and following the land use source classification scheme, RED and H_{RGB} exhibited significant variability and this was fundamental in achieving more reliable source discrimination, increasing by 17% and 13%, the respective values of Wilks' Lambda and the samples correctly classified by LDA. Unlike soils under natural vegetation in humid and cold environments, soils under Caatinga did not show colour indices associated with darker shades. Most species of this vegetation lose their leaves during a significant part of the year, mainly at the end of the rainy season and at the beginning of the dry season. However, these climatic conditions, and especially temperature and relative humidity, do not facilitate the accumulation of organic matter in these soils (Costa et al., 2010; Lima et al., 2015; Holanda et al., 2017). The rotation with agricultural activities, mainly agropastoral, and the lower biomass production of mostly xerophytic species, compared to natural wetland species, may also be responsible for this pattern (Almagro et al., 2015; Wiesmeier et al., 2019).

4.2 Sediment source contribution patterns under semiarid environmental conditions

The lower catchment contributed most of the sediment to the outlet of the investigated river system; approximately 69% and 56% of SS and BS, respectively. Low connectivity along the main stream may be responsible for promoting this pattern. Dams have been built over recent decades, modifying the dynamics of sediment redistribution and longitudinal connectivity (CONDEPE / FIDEM, 2005). The different rainfall regimes may also contribute as the annual rainfall increases from the upper to lower catchment (CONDEPE / FIDEM, 2005).

The average contributions of the upper catchment (SS = 23%; BS = 33%) were two-three fold greater than those estimated for the middle catchment (SS = 8%; BS = 10%). Typically, sources collected at larger distances from target sediment collection points have lower contributions because of the longer travel pathways and times (Le gall et al., 2017; Silva et al., 2018a; Batista et al., 2019). Such effects are likely pronounced in our study basin due to the following reasons: 1) the presence of small dams; 2) the longer transport times in semiarid compared with humid environments, and; 3) the flattened shape of the basin. It is important to note that although the shape of the studied catchment results in a short distance from source to the main river channel, the lower rainfall regime in the upper part of the catchment may result in a longer period for the eroded soil particles reach the main river channel than in the lower portion of the catchment. Even though, some overestimation of the sediment contributions from the upper catchment may have occurred because of the close similarity of the geochemical properties of this zone with those found in the lower catchment, as observed for Co, Cr, Ni, and V and the corresponding LDA results (Figure 2). Gneisses and orthogneisses represent both of these two regions since they cover more than 62% of the upper catchment and almost all of the slope-channel connected areas in the lower catchment (Figure 1).

Overall, the Caatinga contribution (SS = 49%; BS = 47%) was slightly higher than that of channel banks (SS = 35%; BS = 39%) (Figure 4). Lower contributions from the Caatinga were expected here, due to its well-developed vegetation cover. On the one hand, in field experiments with simulated rainfall on soils under semiarid conditions, this vegetation type promoted similar or significantly lower rates of interril erosion than areas under cultivation and bare soil (Cantalice et al., 2019; Cantalice et al., 2021). On the other hand, the combination of various factors may have contributed to our source apportionment results: (1) the vegetation of the Caatinga biome covers the river basin almost entirely; also, it is often formed by secondary forest under initial or intermediate regeneration, characterized by shrubby plants with larger intervening spacing and during part of the year these plants lose their leaves reducing interception (Costa et al., 2010; Lima et al., 2015; Holanda et al., 2017; Menezes et al., 2021); (2) the rainfall in this region is typified by high-intensity regimes generating fast hydrological responses, minimizing the protection afforded by this type of native vegetation against erosion (Medeiros et al., 2014; Silva et al., 2015), and; (3) the widespread accumulation of sodium in soils may promote the dispersion of soil particles, thereby facilitating sediment mobilization in runoff (Souza et al., 2014).

The riparian vegetation does not protect channel banks sufficiently and did not result in low relative sediment contributions from channel banks (Silva et al., 2016; Devi et al., 2019). Here, channel banks correspond to deep walls incised by the river network, typically varying between 3-8 m in height. These morphological features can minimize root protection and lead to high erosion rates similar to degraded channel banks (Tiecher et al., 2018; Amorim et al., 2021). In contrast, unpaved roads were estimated to make lower contributions (SS = 16%; BS = 13%) to the sampled target sediment. The smaller relative area of unpaved road surfaces and their lower connectivity to the channel system may explain this result. Similarly, low sediment contributions from unpaved roads have also been reported for large river basins under humid climates (Tiecher et al., 2018; Ramon et al., 2020; Amorim et al., 2021).

Conclusions

The recovery and conservation of the vegetation in the Caatinga biome and the stabilization of channel banks, especially in the lower catchment, are fundamental to controlling the sediment problem in our semiarid study catchment. Poor conservative behaviour is one of the challenges for the application of colour tracers to quantifying sediment sources in this ephemeral river. Nevertheless, such tracers were fundamental for the most reliable sediment source apportionment based on the land use classification scheme. More studies are needed to evaluate the conservative behaviour of colour parameters in semiarid environments, especially at smaller scales. Sampling in smaller basins can better demonstrate sediment delivery dynamics within these environments since the transfer time of sediments is even longer in semiarid environmental conditions than in most humid conditions.

Acknowledgements

Y.J.A.B. Silva are grateful to the National Council for Scientific and Technological Development – CNPq for research productivity scholarships (Process Number: 303221/2019-4). The contribution to this manuscript by ALC was funded by UKRI-BBSRC (UK Research and Innovation-Biotechnology and Biological Sciences Research Council) grant award BBS/E/C/000I0330.

References

Agência Condepe/Fidem, 2005. Rio Ipojuca, Recife. Série Bacias Hidrográficas de Pernambuco, 1.

Almagro, M., Maestre, F.T., Martínez-López, J., Valencia, E., Rey, A., 2015. Climate change may reduce litter decomposition while enhancing the contribution of photodegradation in dry perennial Mediterranean grasslands. Soil. Biol. Biochem. 90, 214-223. https://doi.org/10.1016/j.soilbio.2015.08.006.

Amorim, F.F., da Silva, Y.J.A.B., Nascimento, R.C., da Silva, Y.J.A.B., Tiecher, T., do Nascimento, C.W.A., Minella, J.P.G., Zhang, Y., Ram, H.U., Pulley, S. Collins, A.L., 2021. Sediment source apportionment using optical property composite signatures in a rural catchment, Brazil. Catena. 202, 105208. https://doi.org/10.1016/j.catena.2021.105208.

Ayrault, S., Le Pape, P., Evrard, O., Priadi, C.R., Quantin, C., Bonté, P., Roy-Barman, M., 2014. Remanence of lead pollution in an urban river system: a multi-scale temporal and spatial study in the Seine River basin, France. Environ. Sci. Pollut. R. 21(6), 4134-4148. https://doi.org/10.1007/s11356-013-2240-6.

Batista, P.V., Laceby, J.P., Silva, M.L., Tassinari, D., Bispo, D.F., Curi, N., Davies, J., Quinton, J.N., 2019. Using pedological knowledge to improve sediment source apportionment in tropical environments. J. Soils Sediments. 19(9), 3274-3289. https://doi.org/10.1007/s11368-018-2199-5.

Ben Slimane, A., Raclot, D., Evrard, O., Sanaa, M., Lefevre, I., Le Bissonnais, Y., 2016. Relative contribution of rill/interrill and gully/channel erosion to small reservoir siltation in Mediterranean environments. Land Degrad. Dev. 27 (3), 785-797. https://doi.org/10.1002/ldr.2387.

Cantalice, J.R.B., Nunes, E.O.S., Cavalcante, D.M., Barbosa, B., Junior, G.B., Guerra, S.M.S., Neto, F.R., 2019. Vegetative-hydraulic parameters generated by agricultural crops for laminar flows under a semi-arid environment of Pernambuco, Brazil. Ecol. Indic. 106, 105496. https://doi.org/10.1016/j.ecolind.2019.105496.

Cantalice, J.R.B., Dias, I.C.G.M., Andrade, D.S., Assis Filho, F.M., Souza, W.L.S., Nunes, E.O.S., Junior, G.B., 2021. Hydraulic resistance to overland flow governed by Froude number on semiarid hillslopes under shrubs and crops. Hydrolog. Sci. J. 66(10) 1531-1540, 2021. https://doi.org/10.1080/02626667.2021.1947506.

Collins, A.L., Walling, D.E., Leeks, G.J.L., 1997. Source type ascription for fluvial suspended sediment based on a quantitative composite fingerprinting technique. Catena. 29(1), 1-27. https://doi.org/10.1016/S0341-8162(96)00064-1.

Collins, A.L., Burak, E., Harris, P., Pulley, S., Cardenas, L., Tang, Q., 2019. Field scale temporal and spatial variability of δ13C, δ15N, TC and TN soil properties: implications for sediment source tracing. Geoderma. 333, 108-122. https://doi.org/10.1016/j.geoderma.2018.07.019.

Collins, A.L., Blackwell, M., Boeckx, P., Chivers, C.A., Emelko, M., Evrard, O., Foster, I., Gellis, A., Gholami, H., Granger, S., Harris, P., Horowitz, A.J., Laceby, J.P., Martinez-carreras, N., Minella, J., Mol, L., Nosrati, K., Pulley, S., Silins, U., Silva, Y.J.A.B., Stone, M., Tiecher, T., Upadhayay, H.R., Zhang, Y., 2020. Sediment source fingerprinting: benchmarking recent outputs, remaining challenges and emerging themes. J. Soils Sediments. 20(12), 4160-4193. https://doi.org/10.1007/s11368-020-02755-4.

Costa, C.C.D.A., Camacho, R.G.V., Macedo, I.D.D., Silva, P.C.M.D., 2010. Análise comparativa da produção de serapilheira em fragmentos arbóreos e arbustivos em área de caatinga na FLONA de Açu-RN. Rev. Arvore. 34, 259-265. https://doi.org/10.1590/S0100-67622010000200008.

Devi, T.B., Sharma, A., Kumar, B., 2019. Flow characteristics in a partly vegetated channel with emergent vegetation and seepage. Ecohydrol. Hydrobiol. 19, 93-108. https://doi.org/10.1016/j.ecohyd.2018.07.006.

Correia, R.C., Kiill, L.H.P., de Moura, M.S.B., Cunha, T.J.F., de Jesus Júnior, L.A., Araújo, J.L.P., 2011. A região semiárida brasileira. Embrapa Semiárido-Capítulo em livro científico (ALICE).

Estévez Alvarez, J., Montero, A., Jiménez, N., Muñiz, U., Padilla, A., Molina, R., Quicute de Vera, S., 2001. Nuclear and related analytical methods applied to the determination of Cr, Ni, Cu, Zn, Cd and Pb in a red ferralitic soil and Sorghum samples. J. Radioanal. Nucl. Ch. 247(3), 479-486. https://doi.org/10.1023/a:1010640009301.

Garzon-Garcia, A., Laceby, J.P., Olley, J.M., Bunn, S.E., 2017.Differentiating the sources of fine sediment, organic matter and nitrogen in a subtropical Australian catchment. Sci. Total Environ. 575, 1384-1394. https://doi.org/10.1016/j.scitotenv.2016.09.219.

Holanda, A.C.D., Feliciano, A.L.P., Freire, F.J., Sousa, F.Q.D., Freire, S.R.D.O., Alves, A.R., 2017. Aporte de serapilheira e nutrientes em uma área de caatinga. Cienc. Florest. 27, 621-633. https://doi.org/10.5902/1980509827747.

IPCC - Intergovernmental panel on climate change, 2014. Climate Change 2014: Impacts, Adaptation, and Vulnerability. https://www.ipcc.ch/site/assets/uploads/2018/02/ar5_wgII_spm_en.pdf. (accessed 2 May 2021).

Le Gall, M., Evrard, O., Dapoigny, A., Tiecher, T., Zafar, M., Minella, J.P.G., Laceby, J.P., Ayrault, S., 2017. Tracing sediment sources in a subtropical agricultural catchment of Southern Brazil cultivated with conventional and conservation farming practices. Land Degrad. Dev. 28(4), 1426-1436. https://doi.org/10.1002/ldr.2662.

Lima, R.P., Fernandes, M.M., Fernandes, M.R.D.M., Matricardi, E.A.T., 2015. Aporte e decomposição da serapilheira na Caatinga no Sul do Piauí. Florest. Amb. 22, 42-49, 2015. https://doi.org/10.1590/2179-8087.062013.

Lima Barros, A.M., do Carmo Sobral M., Gunkel, G., 2013. Modelling of point and diffuse pollution: application of the Moneris model in the Ipojuca river basin, Pernambuco State, Brazil. Wat. Sci. Tech. 68(2), 357–365. https://doi.org/10.2166/wst.2013.086.

Marengo, J.A., 2008. Vulnerabilidade, impactos e adaptação do clima no semiárido do Brasil. Parcerias estratégicas. Brasília, DF. N° 27,1-5.

Martínez-Carreras, N., Udelhoven, T., Krein, A., Gallart, F., Iffly, J.F., Ziebel, J., Hoffmann, L., Pfister, L., Walling, D.E., 2010. The use of sediment colour measured by diffuse reflectance spectrometry to determine sediment sources: application to the Attert River catchment (Luxembourg). J Hydrol. 382, 49-63.. https://doi.org/10.1016/j.jhydrol.2009.12.017.

Medeiros, P.H.A., de Araújo, J.C., 2014. Temporal variability of rainfall in a semiarid environment in Brazil and its effect on sediment transport processes. J. Soils Sediments. 14(7), 1216-1223. https://doi.org/10.1007/s11368-013-0809-9.

Menezes, R.S.C., Sales, A.T., Primo, D.C., de Albuquerque, E.R.G.M., de Jesus, K.N., Pareyn, F.G.C., Sampaio, E.V.D.S.B., 2021. Soil and vegetation carbon stocks after land-use changes in a seasonally dry tropical forest. Geoderma. 390, 114943, 2021. https://doi.org/10.1016/j.geoderma.2021.114943.

Minella, J.P.G., Merten, G.H., Reichert, J.M., Santos, D.R., 2017. Identificação e implicações para a conservação do solo das fontes de sedimentos em bacias hidrográficas. Rev. Bras. Cienc. Solo. v. 31, n. 6, p. 1637–1646, 2007. https://doi.org/10.1590/S0100-06832007000600039.

Murphy C.P., 1986. Thin section preparation of soils and sediments. Academic Publishing, Berkhanmsterd (145 pp).

NIST - National Institute of Standards and Technology, 2002. Standard Reference Materials -SRM 2709, 2710 and 2711.

Neto, M.V.B.; de Araújo, M.D.S.B.; de Araújo Filho, J.C.; Sampaio, E.V.D.S.B.; Almeida, B.G., 2020. Rill and sheet soil erosion estimation in an area undergoing desertification in the Brazilian semi-arid region. Model. Earth. Syst. Environ. 1-9. https://doi.org/10.1007/s40808-020-01026-y.

Nosrati, K., Akbari-Mahdiabad, M., Ayoubi, S., Degos, E., Koubansky, A., Coquatrix, Q., Collins, A. L. 2020. Storm dust source fingerprinting for different particle size fractions using colour and magnetic susceptibility and a Bayesian un-mixing model.

Environmental Environ. Sci. Pollut. R. 27(25), 31578-31594. https://doi.org/10.1007/s11356-020-09249-3.

Nosrati, K., Akbari-Mahdiabad, M., Ayoubi, S., Collins, A. L. 2021a. An exploratory study on the use of different composite magnetic and colour fingerprints in aeolian sediment provenance fingerprinting. Catena. 200, 105182. https://doi.org/10.1016/j.catena.2021.105182.

Nosrati, K., Akbari-Mahdiabad, M., Fiener, P., Collins, A.L., 2021b. Using different size fractions to source fingerprint fine-grained channel bed sediment in a large drainage basin in Iran. Catena. 200, 105173. https://doi.org/10.1016/j.catena.2021.105173.

Nosrati, K., Mohammadi-Raigani, Z., Haddadchi, A., Collins, A. L., 2021c. Elucidating intra-storm variations in suspended sediment sources using a Bayesian fingerprinting approach. J Hydrol. 596, 126115. https://doi.org/10.1016/j.jhydrol.2021.126115.

Phillips, J.M., Russell, M.A., Walling, D.E., 2000. Time-integrated sampling of fluvial suspended sediment: a simple methodology for small catchments. Hydrol. Process. 14(14), 2589-2602. https://doi.org/10.1002/1099-1085(20001015)14:14<2589::AID-HYP94>3.0.CO;2-D.

Phillips, D.L., Gregg, J.W., 2003. Source partitioning using stable isotopes: coping with too many sources. Oecologia. 136(2), 261-269. https://doi.org/10.1007/s00442-003-1218-3.

Pulley, S., Rowntree, K., 2016. The use of an ordinary colour scanner to fingerprint sediment sources in the South African Karoo. J. Environ. Manage. 165, 253-262. https://doi.org/10.1016/j.jenvman.2015.09.037.

Pulley, S., Collins, A.L., 2021. The potential for colour to provide a robust alternative to high-cost sediment source fingerprinting: Assessment using eight catchments in England. Sci. Total Environ. 148416. https://doi.org/10.1016/j.scitotenv.2021.148416.

Pulley, S., Collins, A.L. 2022. A rapid and inexpensive colour-based sediment tracing method incorporating hydrogen peroxide sample treatment as an alternative to quantitative source fingerprinting for catchment management. J. Environ. Manage. 311, 114780. https://doi.org/10.1016/j.jenvman.2022.114780.

Ramon, R., Evrard, O., Laceby, J.P., Caner, L., Inda, A.V., De Barros, C.A., Minella, J. P., Tiecher, T., 2020. Combining spectroscopy and magnetism with geochemical tracers to improve the discrimination of sediment sources in a homogeneous subtropical catchment. Catena. 195, 104800. https://doi.org/10.1016/j.catena.2020.104800.

Silva, Y.J.A.B., Cantalice, J.R.B., Singh, V.P., do Nascimento, C.W.A., Piscoya, V. C., Guerra, S.M., 2015. Trace element fluxes in sediments of an environmentally impacted river from a coastal zone of Brazil. Environ. Sci. Pollut. R. 22(19), 14755-14766. https://doi.org/10.1007/s11356-015-4670-9.

Silva, Y.J.A.B., Cantalice, J.R.B., Singh, V.P., Cruz, C.M.C.A., da Silva Souza, W.L., 2016. Sediment transport under the presence and absence of emergent vegetation in a natural alluvial channel from Brazil. Int. J. Sediment. Res. 31(4), 360-367. https://doi.org/10.1016/j.ijsrc.2016.01.001.

Silva, Y.J.A.B., Cantalice, J.R.B., do Nascimento, C.W.A., Singh, V.P., da Silva, Y.J.A.B., Silva, C.M.C.A.C., Silva, M.O., Guerra, S.M., 2017. Bedload as an indicator of heavy metal contamination in a Brazilian anthropized watershed. Catena. 153, 106-113. https://doi.org/10.1016/j.catena.2017.02.004.

Silva, E.M., Medeiros, P., Araújo, J.C.D., 2018a. Applicability of fingerprinting for identification of sediment sources in a mesoscale semiarid catchment. Eng. Agric. 38, 553-562. https://doi.org/10.1590/1809-4430-Eng.Agric.v38n4p553-562/2018.

Silva, Y.J.A.B., do Nascimento, C.W.A, da Silva Y.J.A.B., Amorim, F.F., Cantalice, J.R.B., Singh, V.P., Collins, A.L., 2018b. Bed and suspended sediment-associated rare earth element concentrations and fluxes in a polluted Brazilian river system. Environ. Sci. Pollut. R. 25(34), 34426–34437. https://doi.org/10.1007/s11356-018-3357-4.

Simplício, A.A.F., Costa, C.A.G., Navarro-Hevia, J., de Araújo, J.C., 2020. Erosion at hillslope and micro-basin scales in the Gilbués Desertification Region, North-eastern Brazil. Land Degrad. Dev. https://doi.org/10.1002/ldr.3809.

Souza, E.R., dos Santos Freire, M.B.G., de Melo, D.V.M., de Assunção Montenegro, A.A., 2014. Management of Atriplex nummularia Lindl. in a salt affected soil in a semi arid region of Brazil. Int. J. Phytoremediat. 16(1), 73-85. https://doi.org/10.1080/15226514.2012.759529.

Stock, B.C., Semmens, B.X., 2016. MixSIAR, G.U.I. User Manual. Version 3, 1.

Tiecher, T., Minella, J.P.G., Miguel, P., Alvarez, J.W.R., Pellegrini, A., Capoane, V., Ciotti, L.H., Schaefer, G.L., Santos, D.R.D., 2014. Contribuição das fontes de sedimentos em uma bacia hidrográfica agrícola sob plantio direto. Rev. Bras. Cienc. Solo, 38(2), 639-649. https://doi.org/10.1590/S0100-06832014000200028.

Tiecher, T., Caner, L., Minella, J.P.G., dos Santos, D.R., 2015. Combining visible-based-color parameters and geochemical tracers to improve sediment source discrimination and apportionment. Sci. Total Environ. 527, 135-149. https://doi.org/10.1016/j.scitotenv.2015.04.103.

Tiecher, T., Caner, L., Minella, J.P.G., Bender, M.A., dos Santos, D.R., 2016. Tracing sediment sources in a subtropical rural catchment of southern Brazil by using geochemical tracers and near-infrared spectroscopy. Soil. Till. Res. 155, 478-491. https://doi.org/10.1016/j.still.2015.03.001.

Tiecher, T., Minella, J.P.G., Evrard, O., Caner, L., Merten, G.H., Capoane, V., Didoné, E. J.; Dos Santos, D.R., 2018. Fingerprinting sediment sources in a large agricultural catchment under no-tillage in Southern Brazil (Conceição River). Land Degrad. Dev. 29(4), 939-951. https://doi.org/10.1002/ldr.2917.

Tomasella, J., Vieira, R.M.S.P., Barbosa, A.A., Rodriguez, D.A., de Oliveira Santana, M., Sestini, M.F., 2018. Desertification trends in the Northeast of Brazil over the period

2000–2016. Int. J. Appl. Earth Obs. 73, 197-206. https://doi.org/10.1016/j.jag.2018.06.012.

Uber, M., Legout, C., Nord, G., Crouzet, C., Demory, F., Poulenard, J., 2019. Comparing alternative tracing measurements and mixing models to fingerprint suspended sediment sources in a mesoscale Mediterranean catchment. J. Soils Sediments. 1-19. https://doi.org/10.1007/s11368-019-02270-1.

Viscarra Rossel, R.A., 2004. ColoSol: executable software to perform colour space model transformations for soil colour.

Walling, D.E., Woodward, J.C., 1992. Use of radiometric fingerprints to derive information on suspended sediment sources. In Erosion and sediment monitoring programmes in river basins. Proc. international symposium, Oslo. (pp. 153-164). International Association of Hydrological Sciences.

Wiesmeier, M., Urbanski, L., Hobley, E., Lang, B., Von Lützow, M., Marin-Spiotta, E., Wesemael, B., Rabot, E., Ließ, M., Garcia-Franco, N., Wollschläger, U., Vogel, H., Kögel-Knabner, I., 2019. Soil organic carbon storage as a key function of soils-A review of drivers and indicators at various scales. Geoderma. 333, 149-162. https://doi.org/10.1016/j.geoderma.2018.07.026.